
MAGNETIC

RESONANCE

ANGIOGRAPHY OF

THE HEAD AND NECK

• **A Teaching File** •

• **Jeffrey S. Ross** •

MAGNETIC RESONANCE ANGIOGRAPHY

of the HEAD and NECK: *A Teaching File*

Jeffrey S. Ross, M.D.

Head

Section of Magnetic Resonance Imaging

Department of Radiology

The Cleveland Clinic Foundation

Cleveland, Ohio

with 822 illustrations



Mosby

St. Louis Baltimore Berlin Boston Carlsbad Chicago London Madrid

Naples New York Philadelphia Sydney Tokyo Toronto

Executive Editor: Susan M. Gay
Project Manager: Carol Sullivan Weis
Senior Production Editor: Pat Joiner
Manufacturing Manager: Kathy Grone
Book Designer: Sheilah Barrett

Copyright 1995 by Mosby-Year Book, Inc.

All rights reserved. No part of this publication may be reproduced, stored in a retrieval system, or transmitted, in any form or by any means, electronic, mechanical, photocopying, recording, or otherwise, without prior written permission from the publisher.

Permission to photocopy or reproduce solely for internal or personal use is permitted for libraries or other users registered with the Copyright Clearance Center, 27 Congress Street, Salem, MA 01970, provided that the base fee of \$4.00 per chapter plus \$.10 per page is paid directly to the Copyright Clearance Center. This consent does not extend to other kinds of copying, such as copying for general distribution, for advertising or promotional purposes, for creating collected works, or for resale.

Printed in the United States of America
Composition by the Clarinda Company
Printing/binding by Maple-Vail Book Manufacturing Group

Mosby-Year Book, Inc.
11830 Westline Industrial Drive
St. Louis, MO 63146

Library of Congress Cataloging in Publication Data

Ross, Jeffrey S. (Jeffrey Stuart)

Magnetic resonance angiography of the head and neck: a teaching file / Jeffrey S. Ross.

p. cm.

Includes bibliographical references and index.

ISBN 0-8151-7409-8

1. Cerebrovascular disease—Magnetic resonance imaging. 2. Brain—Blood-vessels—Magnetic resonance imaging. I. Title.

[DNLM: 1. Magnetic Resonance Imaging—methods. 2. Angiography—methods—case studies. 3. Head—anatomy & histology. 4. Neck—anatomy & histology. 5. Cerebrovascular Disorders—diagnosis—case studies. WN 445 R824m 1994]

RC388.5.R686 1994

616.8'107548—dc20

DNLM/DLC

for Library of Congress

94-31810
CIP

MAGNETIC RESONANCE ANGIOGRAPHY

of the HEAD and NECK: *A Teaching File*



Volumes in the *Teaching File Series*

- IMAGING of CNS DISEASE: A CT and MR TEACHING FILE
Douglas H. Yock, Jr.
- ALIMENTARY TRACT IMAGING: A *Teaching File*
C. Daniel Johnson
- NUCLEAR MEDICINE: A *Teaching File*
Frederick L. Datz
Gregory G. Patch
John M. Arias
Kathryn A. Morton
- RADIOLOGY of THORACIC DISEASES: A *Teaching File*
Stephen J. Swensen
- MAGNETIC RESONANCE ANGIOGRAPHY of the HEAD and NECK: A *Teaching File*
Jeffrey S. Ross
- MAGNETIC RESONANCE IMAGING of CNS DISEASE: A *Teaching File*
Douglas H. Yock, Jr.



Where is the wise man? Where is the scholar? Where
is the philosopher of this age? Has not God made
foolish the wisdom of the world?

1 Corinthians 1:20

PREFACE

Tremendous changes have taken place in hardware and software since my first involvement in the infant stages of MRA in 1987. Improvements such as shorter echo times, improved motion compensation, and faster and more user-friendly reconstructions have allowed MRA to become a mainstream, if not a prerequisite, part of the evaluation of a variety of neuropathologies. It is hard to imagine a complete evaluation of the cerebrovasculature without some element of MRA or the intracranial circulation or carotid bifurcation. However, MRA is not an easy modality to learn, since it requires the combined knowledge of MR, with its variety of artifacts, and neurovascular anatomy.

The purpose of this book is to try to help in that learning process of MRA by providing a variety of case material in a straightforward manner, with appropriate references and discussion of pathologic processes. The first chapter is an introduction to the concepts involved in MRA with a purposely "non-physics minded" approach. I apologize for the one equation that did slip in. The second chapter, which is supplemented with line drawings of the sequence setups, is devoted to the wide variety of techniques available and should be referred to if there is a question about individual case parameters in the other chapters. Each chapter covering specific pathologic processes begins with an introductory section, explaining the pathology or imaging considerations. The remainder of each chapter is a series of cases with illustrative MR imaging and MRA images and correlative conventional angiography or computed tomographic images. Because of the tremendous variety of hardware and software available, I have placed emphasis on different MRA techniques used by placing the parameters at the beginning of each case, along with a short history. The cases are set up so that, in general, the reader can first test his or her knowledge by evaluating the images, with the diagnosis, discussion, pertinent figures, and references available once the reader has arrived at the differential diagnosis. Although a wide variety of pathologies are certainly covered, I have also attempted to provide different views of the same pathologic process. This is particularly true of the chapter on the carotid bifurcation, which provides many variations

on the theme of atherosclerosis but with a variety of techniques, parameters, and views of this important MRA area. Although there is discussion of different pathologies presented in this series of teaching cases, this book is *not* meant as an all-encompassing primer on cerebrovascular disease, nor is it meant to supplant the current excellent textbooks on MR imaging. It is meant to serve as a complement to those works, with a particular emphasis on MRA and the unique problems MRA presents. Some of those problems are highlighted by the pitfall cases at the beginning of chapters. Since MR is such a dynamic technology, it is difficult to remain state of the art with the necessary production schedule of a book. Nevertheless, I have attempted to use mainstream or almost mainstream techniques in this series. The time-of-flight and phase-contrast techniques and underlying physical principle will remain the same regardless of the specific machine or field of strength used.

Acknowledgments

I would like to extend thanks to the radiologists who so graciously gave me access to their case material and without whom this book could not have been completed.

John Huston, III, M.D.

Walter Kucharczyk, M.D.

John Sherman, M.D.

Alison S. Smith, M.D.

And, of course, a special thanks to my friends colleagues at the Cleveland Clinic who gave invaluable time and input into the substance of the text and images, and put up with my scavenging for cases.

Paul Ruggieri, M.D.

Micheal T. Modic, M.D.

Thomas J. Masaryk, M.D.

Jean Tkach, Ph.D.

Robert Wallace, M.D.

John Perl, M.D.

To Peg, Whitney and Tyler, my earthly foundation.

Jeffrey S. Ross

INTRODUCTION

A similar convention regarding MRA techniques will be used throughout the book, with the following format as an example:

Technique #1: Carotid (1.0 T) / axial volume three-dimensional time-of-flight, 40/11/25, 256 × 256, 64 partitions, 80-mm slab, 20-cm field of view, 10:57. Echo time is prolonged relative to the usual 7-ms echo time at 1.5 T, since fat and water cycle inphase at 1.0 T with 7-ms echo time and opposed phase at echo time of 11. Prolonging the

echo time to opposed phase improves background sufficiently to outweigh the increased dephasing that might occur.

Technique #2: Intracranial / axial volume, three-dimensional time-of-flight, 40/7/15, 256 × 256, 64 partitions, 80-mm slab, 20-cm field of view, 10:57.

EXPLANATION

Carotid	Cervical carotid artery protocol
Intracranial	Intracranial circulation protocol
axial volume	Orientation of individual partition (i.e., axial, sagittal, or coronal).
40/11/25	Repetition time / echo time / flip angle.
256 x 256	In-plane matrix size
64 partitions	Number of slices acquired for a two-dimensional sequence or in a three-dimensional data set


80-mm slab	Thickness of imaging volume; thickness ÷ number of partitions = slice thickness
10:57	Total imaging time (minutes:seconds).

All time-of-flight sequences have velocity compensation in read and slice and one excitation (acquisition) unless otherwise noted. Intracranial arterial MRAs uniformly have a superior saturation pulse.



CONTENTS



- 1 BASIC PRINCIPLES, 1
 - 2 TECHNIQUES, 13
 - 3 NORMAL ANATOMY, VARIANTS,
and CONGENITAL ANOMALIES, 41
 - 4 ANEURYSMS, 79
 - 5 VASCULAR MALFORMATIONS, 163
 - 6 INTRACRANIAL STENOSIS and
OCCLUSION, 203
 - 7 TUMORS and VASCULAR LOOPS, 264
 - 8 VENOUS DISEASE (EXCLUDING
VASCULAR MALFORMATIONS), 293
 - 9 CAROTID BIFURCATION, 313
 - 10 DISSECTION, 373
- 

Basic Principles

Magnetic resonance angiography (MRA) has been applied to several manifestations of cerebrovascular disease. Although these methods are powerful for demonstrating pathologic conditions, the clinician must keep their limitations in mind so that the appropriate method is applied to answer a specific clinical question and that the acquisition parameters are chosen to maximize the sensitivity and specificity of the study. After choosing the appropriate technique, the clinician must decide whether the conventional parenchymal MR imaging and MRA evaluation are sufficient in a particular clinical setting or whether a more traditional, invasive angiographic study is necessary. For the central nervous system, MRA studies and flow-measurement techniques compliment the more traditional spin-echo evaluation of patients with aneurysms, arterial and venous stenoses and occlusions, vascular malformations, and occasionally, neoplastic vascular invasions. When carefully defined protocols are used and attention to detail occurs, this new information and improved diagnostic sensitivity can be used routinely, with only minor increases in examination time.

GENERAL TECHNIQUES

Before details of MRA sequences are discussed, some general terms must be defined. A generic spin-echo diagram is shown in Fig. 1-1, with G_z (slice-select), G_y (phase-encode), and G_x (frequency-encode or "read") gradients shown. A similar schematic for a generic gradient-echo sequence is shown in Fig. 1-2. It is assumed that the fundamentals of MR image production are known to the reader, and a detailed explanation is beyond the scope of this book.

Three-Dimensional MR Imaging

In three-dimensional (3D) gradient-echo imaging, a thick slab of interest is defined by the initial radiofrequency (rf) excitation pulse rather than a thin slice, as in two-dimensional (2D) imaging. This volume of tissue is divided into thin, contiguous partitions (slices) by an additional direction of phase encoding along the slice-select direction.

The in-plane phase and frequency-encoding gradients are applied as in 2D imaging. With phase encoding used in two different directions, the imaging time is proportionally increased by the number of slices selected (the additional phase-encoding steps) compared with the imaging time of 2D techniques. Imaging time is therefore equal to the following:

$$\begin{aligned} &\text{Repetition time (TR)} \times \text{Number of excitations} \\ &\quad \times \text{Number of in-plane phase-encoding steps} \\ &\quad \times \text{Number of slices (slice-select phase encoding)} \end{aligned}$$

Although 3D Fourier transform imaging is possible with spin echo (SE) sequences, for all practical purposes, the short TRs achieved by gradient-echo imaging have allowed more widespread applications. Two types of 3D imaging can be used relative to the type of rf pulses utilized: The entire sensitive volume of the surface coil can be used (non-selective), or only a smaller specific volume of tissue can be imaged within the active area of the coil (selective).

The following are theoretical and practical advantages of 3D imaging:

1. There is an increase in the signal-to-noise ratio over 2D imaging, which is the square root of the number of partitions (slices) selected, because of reexcitation of the entire volume with each rf pulse or for every phase-encoding step in each of the two directions. This may be considered analogous to increasing the number of acquisitions in 2D imaging. It is therefore advantageous to increase the number of slices with this technique and increase the area covered.
2. Thin, contiguous slices can be obtained from the volume without the problem of cross-talk found in 2D imaging. (Cross-talk between adjacent 2D slices gives unwanted changes in image contrast from slice to slice and reduces the signal-to-noise ratio because of saturation of the peripheral spins in the slices.) Thinner and more accurate slices can be achieved with 3D techniques because slice thickness depends not on the fidelity of the rf profile but rather on the process of phase encoding. Minimum slice thickness is approximately 0.5 mm for 3D vs. 2.5 mm for 2D imaging.

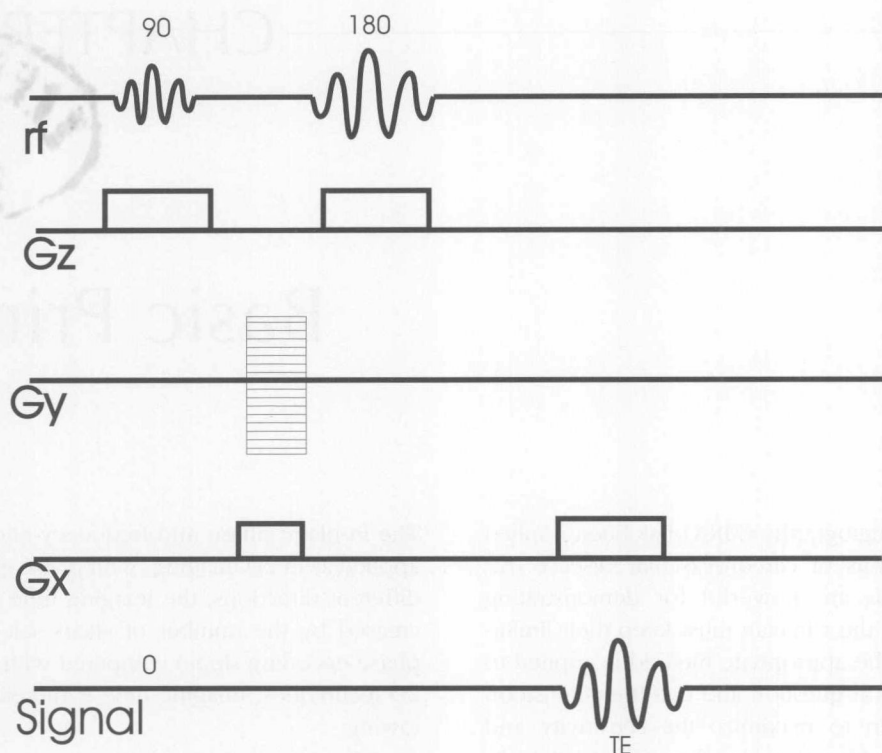


Fig. 1-1 Diagram of conventional spin-echo sequence. The 90- and 180-degree rf pulses are followed by acquisition of the spin echo at the echo time (TE). Three orthogonal magnetic field gradients are used in MR imaging to pinpoint the voxels in space (spatially encode). These gradients—frequency encoded (G_x), phase encoded (G_y), and slice select (G_z)—are produced by electromagnetic coils within the housing of the magnet. The frequency-encoded gradient is also called the *read gradient*.

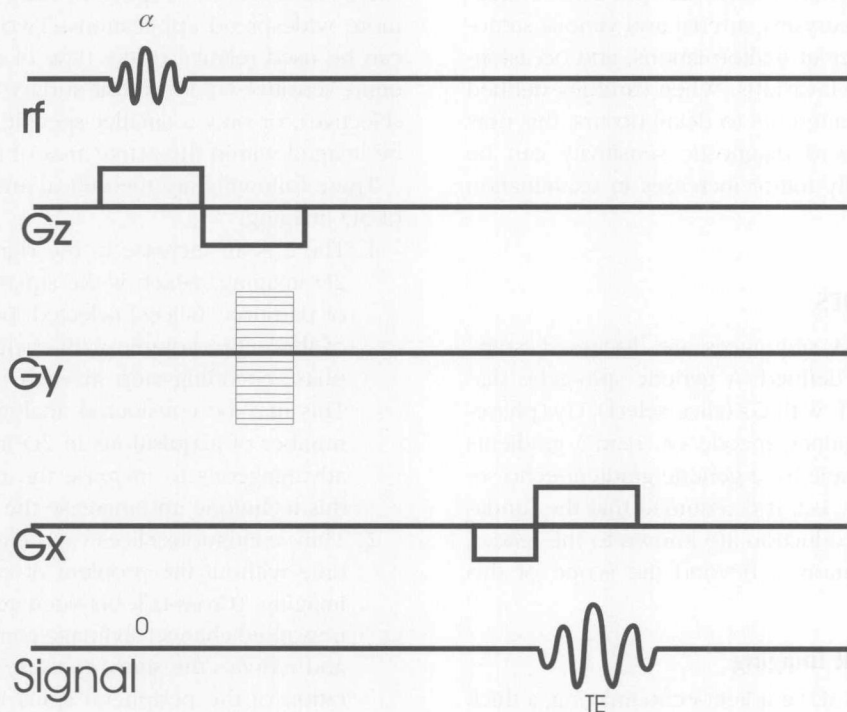


Fig. 1-2 Gradient-echo diagram (2D). Note that the 180-degree rf pulse present in the spin-echo diagram is now missing, with the refocusing produced by the bipolar read gradient (the gradient is applied in one direction, followed by an inverted gradient). One of the advantages of this is a much quicker acquisition time because of shortened TRs in the absence of the necessity of a 180-degree rf pulse. α , Flip angle.

3. The 3D techniques have a reduction in susceptibility artifacts (i.e., T_2^* effects). Susceptibility artifacts can cause false "expansion" of bone at bone-soft tissue-air interfaces, which can result in loss of adjacent vascular signal. Susceptibility artifacts occur when there is apposition of different tissues or air with different magnetic susceptibilities, resulting in the creation of local gradients that in turn produce spin dephasing and T_2^* signal loss. With smaller voxels, there is less tissue heterogeneity within the voxel and less signal loss.
4. Because a volume of data is collected, computer post-processing allows reformatting of the data along any desired imaging plane.

A problem with 3D imaging is truncation artifact (Gibbs artifact) in the in-plane direction (as in 2D) and in the slice-encoding direction because of finite sampling. Ghosting artifacts from motion are present not only along the in-plane phase-encoding directions (as in 2D imaging), but also along the additional direction of phase encoding in slice select. Gross motion artifacts are the most commonly encountered problems affecting the diagnostic quality of 3D techniques because of this sensitivity to motion and the longer acquisition times that make it more difficult for the patient to remain still throughout the examination. Magnetic susceptibility effects associated with the gradient-echo technique may also cause artifacts that are reduced or eliminated in spin-echo sequences. The rf profiles associated with selective and nonselective 3D sequences are not perfect. Although the individual slice thickness is preserved in 3D, the imperfect slice profile may result in excitation of matter outside the volume of interest, with subsequent aliasing of the information into the region of interest. The amount of slice-select aliasing for a fixed volume decreases as the number of partitions increases. The imperfect slice profile also causes nonuniform distribution of the flip angle across the volume and thus nonuniform contrast and signal-to-noise ratio from slice to slice. Although this may not be noticeable on one slice, it can degrade the quality of multiplanar reformats with a banding pattern.

Blood Flow Signal

The signal of blood in MR imaging is roughly related to two aspects of the imaging process. The first is the pulse sequence itself, with variables such as slice orientation, repetition time, and flip angle. This is also called the *time-of-flight (TOF) effect*. TOF effects can increase or decrease vascular signal.¹⁻³ Spins (blood protons) must receive both the 90- and 180-degree rf pulses to be detected and included in the resultant image. TOF effects that decrease the signal of moving blood result from spins that do not remain within the selected imaging slice long enough to be acted on by both rf pulses used in conventional spin-echo imaging (see Figure 1-2). Blood that received a 90-degree pulse and then flowed out of the imaging plane before receiving the 180-degree pulse does not give a signal. Similarly, blood that flows into the imaging slice after the 90-degree pulse and

thus receives only the 180-degree pulse does not give a signal and appears black on the MR image (a flow void).

TOF effects may also produce increased signal intensity of flowing blood, which is the basis for TOF MRA using gradient-echo imaging. Protons placed within a magnetic field tend to orient parallel to the magnetic lines. In routine gradient-echo MR imaging, an rf pulse that flips this vector of magnetization into the transverse plane is applied so that a signal can be detected. With time and if it is left undisturbed, the vector of magnetization grows back longitudinally parallel to the main magnetic field. If another rf pulse is delivered before this growth has occurred, the total detectable signal is decreased. An understanding of this concept is necessary to appreciate how flowing blood can give high signal on MR imaging. *Paradoxical enhancement*, *flow-related enhancement*, and *entry-slice phenomenon* are terms that generally refer to the same phenomenon: Blood moving into an imaging slice not previously exposed to rf energy can show high signal intensity. For conventional gradient-echo imaging with short repetition times, the stationary tissue within the imaging slice receives multiple rf pulses during image acquisition. The protons in this stationary tissue are called *partially saturated* because the repeated rf pulses have not allowed their longitudinal magnetization to recover completely. Spins that have recovered all their magnetization between rf pulses are called *unsaturated*, or *fully magnetized* or *fresh*. Unsaturated blood moving into the image slice can give a relative increase in signal intensity with subsequent applications of rf energy, which is flow-related enhancement.⁴

The second aspect of the imaging process that greatly influences the signal intensity of blood is the signal localizing gradients.⁵⁻⁷ Blood flowing within an imaging plane demonstrates low signal intensity, since spins moving along a magnetic gradient rotate slower or faster depending on the gradient strength to which they are exposed (accumulate a phase change) with respect to stationary tissue. This phase change means that the spins do not rotate coherently. This loss of coherence causes loss of signal. Phase coherence might be compared to a rotating light. A tightly collimated light (such as a laser) has great intensity compared with the same light when it is allowed to disperse randomly around 360 degrees (like a regular light bulb). Phase change or loss of coherence may occur by blood motion along any of the three localizing gradient planes. This process is also called *spin dephasing* or *phase dispersion*.⁸

The factors that influence TOF angiography can therefore be grouped into two categories, each with three important components. The two main factors are *flow-related enhancement* and *phase dispersion*. Achieving the best possible MRA requires the maximization of flow-related enhancement and the minimization of phase dispersion. Factors that affect flow-related enhancement are geometry (slice or slab orientation with respect to the major direction of blood flow, TR, and flip angle). Vessel geometry is a very important consideration in TOF MRA so that high vascular signal can be maintained. In the ideal TOF geometry,

the vessel is perpendicular to the imaging slice, which maximizes flow-related enhancement and minimizes saturation of blood. The main disadvantage of this technique is that it is difficult to cover large vessel lengths with axial 2D slices or 3D volumes. The TR should be long enough to allow full replacement of moving spins by unsaturated spins in the slice to give high vascular signal. The trade-off is that a longer TR allows regrowth of the longitudinal magnetization from the background tissue, which increases background signal intensity. Again, a balance must be struck between increased flow-related enhancement with a longer TR and potentially decreased vessel-soft tissue conspicuousness because background tissue also increases in signal. The appropriate flip angle is a compromise. A higher flip angle gives better signal-to-noise ratio and better suppression (saturation) of the background tissue. It also causes increased saturation of the blood flowing into the slice or slab; that is, the flowing spins become saturated with fewer rf pulses because of the higher flip angle used.

Factors that affect phase change (dispersion) are described later (echo time [TE], voxel, gradients). The phase change that occurs across a voxel is critical to understanding the methods used in MRA to increase vascular signal and may be approximately described by the following:

$$\text{Phase change} = \gamma \text{TE}^2 \cdot G \cdot \Delta V (X \rightarrow) \quad 1-1$$

Where γ is the gyromagnetic ratio, a constant specific for each nuclear species; G is the gradient magnetic field strength; ΔV is the velocity change across a voxel; and X is the directional vector.

This simplified equation describes the factors that can be manipulated to decrease the phase change of moving spins, which would increase vascular signal. All three of the parameters (G , V , TE) are usually manipulated together in MRA. For the sake of clarity, these factors are now be considered separately.

Echo Time

The potential of MRA achieved widespread interest in 1982, when projection MRAs using short TE sequences with cardiac gating were demonstrated.⁹⁻¹¹ As shown in Equation 1-1, TE exerts a powerful effect on the phase change of a moving blood proton. Achieving as short as possible a TE reduces the signal loss associated with motion-induced loss of phase coherence of spins. With a short TE, there is less time for spins to dephase between the time of the excitation pulse and the application of the read gradient. However, depending on the individual hardware, there are physical limits on the shortest TE that can be used secondary to the available gradient strengths (given in mTesla/meter) and gradient rise and fall times (given in milliseconds).

Wedeen et al⁹ were the first to use very short TEs to make projective (thick-slice) arteriograms. In their scheme, two separate sequences were performed, one with high vascular signal and the other with low vascular signal. The stationary soft tissues were the same on each scan, so when

they were subtracted, only the vessels were apparent. The high-vascular-signal scan used short TEs coupled to cardiac gating in diastole. The slow blood flow in diastole allowed minimal phase change of spins, which gave high vascular signal. The low-vascular-signal images had the short TEs but were gated in systole, where the short TE by itself could not overcome the signal loss associated with high-velocity blood flow. In this way, they were able to manipulate TE and V in Equation 1.

Effect of Echo Time on Fat Signal Intensity

It would seem that the shortest possible TE should always be used for MRA. This is not the case in routine clinical imaging for two reasons. A major reason is the interplay between TE and motion compensation gradients (discussed later). The other reason is related to chemical shift. The hydrogen nuclei of fat and water have different environments that cause different precessional frequencies (in fact, a 220-Hz difference at 1.5 Tesla [T]). In spin-echo imaging, the chemical shift effects and field inhomogeneities are mollified by the spin-echo 180-degree refocusing pulse. However, in gradient-echo imaging used in MRA, the spin echo is not present, so fat and water cycle in and out of phase related to the TE and field strength. This cycling from in to out of phase is 3.4 msec/T (every 2.26 msec at 1.5 T and every 3.4 msec at 1.0 T) (Table 1-1). In MRA the quality of images is improved with extraneous fat signal suppression, which is achieved by selecting an appropriately short TE. The shortest opposed phase echo should be used for MRA. For 1.5 T, a 6.5- to 7-msec TE is good, since it is very close to the precise opposed phase TE of 6.78 msec. Transferring this exact MRA sequence to a 1.0-T machine may give inferior image quality because the 7-msec TE would be close to the maximum in-phase echo of 6.8 msec. In this case, prolonging the TE to approximately 10 msec on a 1.0-T machine may improve image quality, since fat is then suppressed. In this example, the worsened phase dispersion present with the longer TE must be compared to the improved suppression of fat with improved postprocessed image quality (Fig. 1-3).

Gradients

Some term definitions are also necessary before discussion of gradient-motion compensation schemes. The rate of change of a moving particle (blood) is its velocity (i.e., distance \div time), or first-order motion. The rate at which a spin's velocity changes is its acceleration, or second-order motion. Similarly, the rate at which a spin's acceleration changes is third-order motion, or jerk. Rates of motion

TABLE 1-1 Timings for In-phase and Opposed Imaging at 1.0 and 1.5 T

T	TE(msec)					
1.0	0	3.4	6.8	10.2	13.6	16.9
1.5	0	2.26	4.52	6.78	9	11.3
		In phase	Out	In	Out	Out

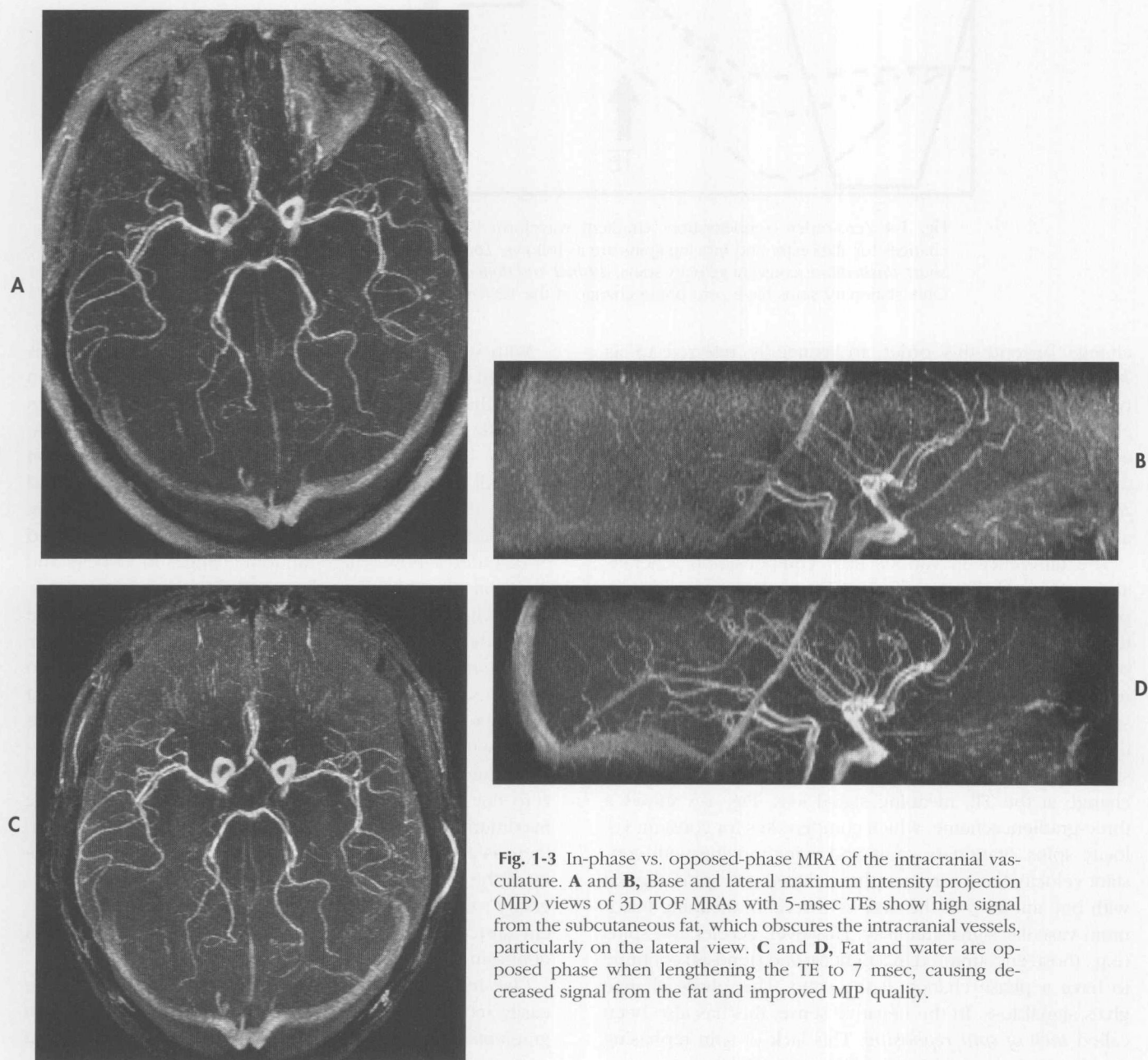


Fig. 1-3 In-phase vs. opposed-phase MRA of the intracranial vasculature. **A** and **B**, Base and lateral maximum intensity projection (MIP) views of 3D TOF MRAs with 5-msec TEs show high signal from the subcutaneous fat, which obscures the intracranial vessels, particularly on the lateral view. **C** and **D**, Fat and water are opposed phase when lengthening the TE to 7 msec, causing decreased signal from the fat and improved MIP quality.

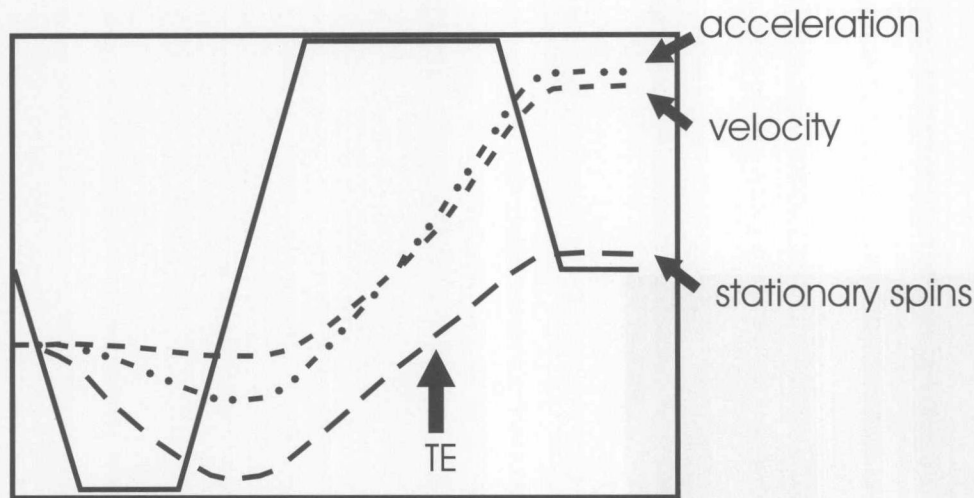


Fig. 1-4 Zero-order compensation. Gradient waveform is shown in a solid line. Phase changes for stationary and moving spins are as follows: *Long, dashed line*, stationary spins; *short, dashed line*, constant velocity spins; *dashed and dotted line*, constant accelerated spins. Only stationary spins have zero phase change at the TE (arrow).

change beyond this order are generally referred to as *higher-order motion*, without specific names. Moran¹² first proposed the use of special gradients to modify the phase changes produced by blood moving along one of the three encoding gradients.¹²⁻¹⁷ These compensation gradients (also called *gradient moment nulling*, *gradient motion re-focusing*, and *flow compensation*) are most commonly used along the read and slice-select gradients.

The difference in various flow compensation schemes along the read direction for gradient-echo imaging is depicted in Figs. 1-4 through 1-6. The vertical axis displays the gradient magnitude (*solid line*) and the phase change of various spins (*dashed lines*), and the horizontal axis represents time. Fig. 1-4 depicts a simple bipolar gradient scheme, which will give zero phase change at the time of the echo for *only* stationary spins. Spins moving with a constant velocity or acceleration continue to have a net phase change at the TE, meaning signal loss. Fig. 1-5 shows a three-gradient scheme, which compensates for constant velocity spins. Stationary spins and spins moving with constant velocity have zero net phase change (all spins aligned with one another) at the time of the echo, meaning maximum vascular signal intensity. However, accelerated spins (e.g., those encountered in a tight carotid stenosis) continue to have a phase change at the echo. This phase change gives signal loss. In the negative sense, this has also been called *lack of spin rephasing*. This lack of spin rephasing may be related to at least the following factors:

1. The velocity compensation scheme has failed to sufficiently refocus the spins with higher-order motion such as acceleration, jerk (the derivative of acceleration), and turbulence.
2. The voxel size is finite.
3. The effects of flow are not compensated in the other two orthogonal planes.

The effect of voxel size is examined in more detail later.

With severe vessel stenosis, an acceleration of blood is required to maintain overall blood flow.¹⁶ This acceleration along the localizing gradients leads to subsequent spin dephasing and signal loss. Further, turbulent flow distal to stenotic lesions results in randomly oriented spin motion along all three imaging planes, which cannot be rephased with gradient correction schemes in only one or two planes. For clinical MRA, turbulence can be thought of as disturbed or disordered flow where random changes in velocity and direction (in addition to the usual flow dynamics) occur. These changes are random or chaotic because the time in which they occur is shorter than the image acquisition time and the distances are shorter than the image resolution. To compensate for velocity and acceleration spin changes, a four-lobe gradient scheme may be implemented (Figure 1-6). With this sequence, spins moving with constant velocity and acceleration, as well as stationary spins, have zero net phase change at the time of the echo, meaning maximum signal intensity (at least theoretically). However, there is a significant drawback of increasing the complexity of the compensation schemes: the much longer TE necessary to provide time for the implementation of the gradient structure. With increasing TE comes increased spin dephasing and signal loss.

One might think that maximal vascular signal could be easily achieved by velocity- and acceleration-compensation gradients in all three orthogonal directions, as well as by a very short TE. However, there is a definite trade-off between TE and the use of compensation gradients. Ever more complex gradient refocusing places demands on the system hardware because gradients must be turned on and off many times within milliseconds of each other. Because these additional gradients must be applied between the rf pulse and the readout period, increasing the gradient compensation scheme also means increasing the TE. Therefore a balance must be struck between the rephasing gained by

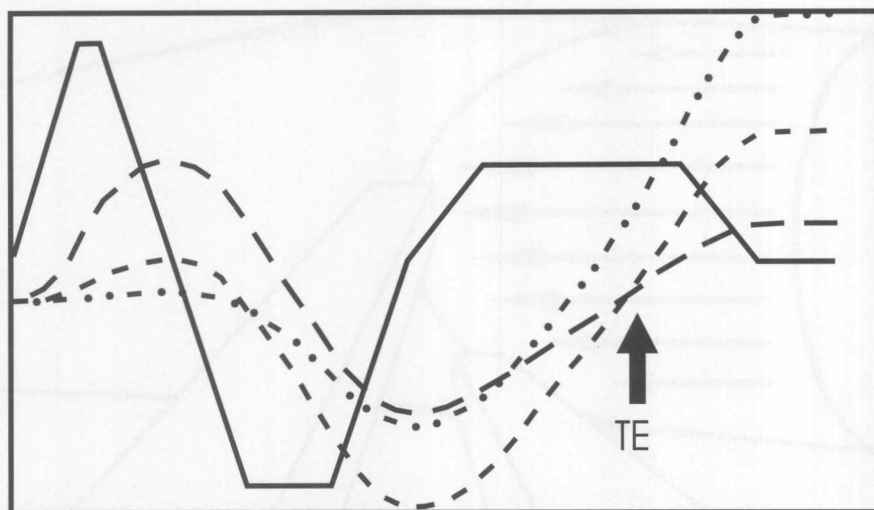


Fig. 1-5 First-order compensation. At the TE (arrow) the stationary and constant-velocity spins have zero phase change while the accelerated spins are not refocused. *Long, dashed line*, stationary spins; *short, dashed line*, constant velocity spins; *dashed and dotted line*, constant accelerated spins.

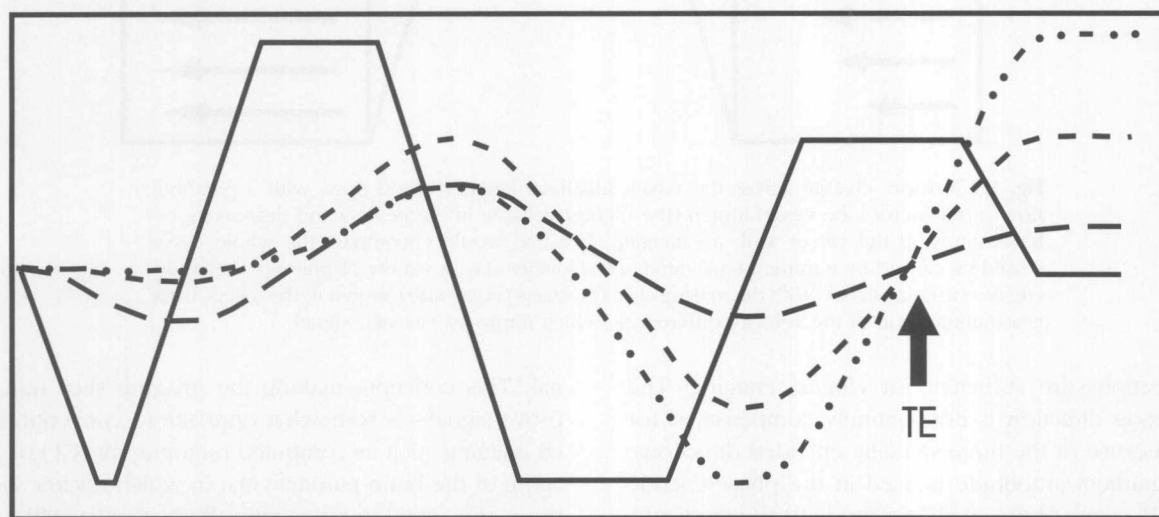


Fig. 1-6 Second-order compensation. At the TE, stationary, constant-velocity, and accelerated spins have been refocused and have zero phase change. The overall length of the gradients must be increased to accommodate the complex gradient waveform, which necessarily increases the TE. (In these sequences, the TE is not in the center of the last gradient lobe by design.) *Long, dashed line*, stationary spins; *short, dashed line*, constant velocity spins; *dashed and dotted line*, constant accelerated spins.

the compensation gradients (increased vascular signal) and the dephasing occurring because of the increased TE (decreased vascular signal). For example, one comparison study of a three-gradient-lobe, velocity-compensated TE, 22-msec sequence with a four-gradient-lobe, velocity- and acceleration-compensated sequence (TE 34 msec) showed no discernible difference in images of the carotid bifurcations in healthy adults.¹⁸ Although the TEs for this study are long compared with those in current sequences, the principle remains the same: The longer TE of the velocity- and

acceleration-compensated sequence negates the advantage of the compensation gradients. This effect of TE should also be true for 2D and phase-contrast applications. Both of these 3D techniques had considerable drawbacks, including susceptibility to patient motion, overlap of the carotid image with the jugular vein, and inability to image carotid stenoses reliably. In 3D TOF angiography, the effect of TE becomes predominate, and it is more important to maintain a short TE with less complex motion refocusing. In general, velocity compensation in the frequency and slice-

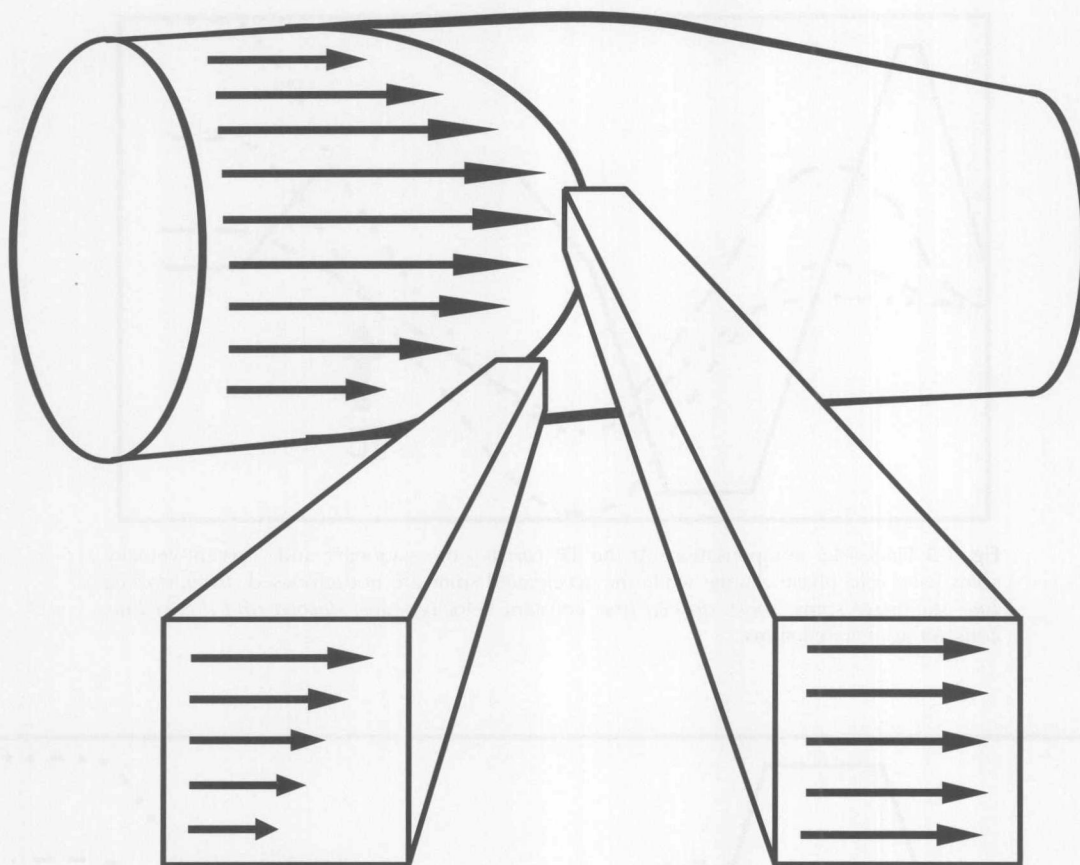


Fig. 1-7 Velocity change across the voxel. Idealized laminar blood flow, with a parabolic flow profile across the vessel lumen (the highest velocity in the center) and decreasing velocities toward the vessel wall. An imaging slice that would encompass the whole vessel would be caused by a tremendous variety of velocities (i.e., a variety of phases), which decreases vascular signal. With decreasing slice thickness (voxel size) shown in the insets, there is a minimization of the velocity differences, which improves vascular signal.

select directions are sufficient for clinical imaging. The phase encode direction is not routinely compensated for motion. Because of the three spatially encoded directions, the least gradient amplitude is used in the phase-encode direction. Because of the small amplitude of the gradients, little phase dispersion occurs along this direction. Also, the duration of this gradient is very short, and it can be placed immediately before the readout period to minimize spatial misregistration. Again, the trade-off of making the gradients longer to accomplish motion correction defeats the purpose when the gradients do not contribute substantially to dephasing.

Velocity Change Across the Imaging Voxel

Idealized blood flow in a vessel may be considered as laminar, with a parabolic flow profile across the vessel lumen and the highest velocity in the center. Any imaging voxel that spans the vessel will encounter a variety of velocities (i.e., a variety of phases). This variety tends to cancel vascular signal if not compensated. This is termed *in-travoxel dephasing*. The spectrum of velocities occurring across an imaging voxel may be minimized by making the voxel smaller (Fig. 1-7). Minimizing the velocity change causes less phase cancellation and improved vascular sig-

nal. This concept—making the imaging slice thin to improve signal—is somewhat opposite to conventional digital imaging such as computed tomography (CT) or MR imaging of the brain parenchyma, in which thicker slices improve the signal-to-noise ratio. With vascular MR imaging, thinner slices are more effective in gaining signal from moving spins because of this decreased phase dispersion and may outweigh the decreased signal-to-noise ratio.¹⁹ One way to decrease this voxel phase change is by using 3D volume imaging instead of the more conventional multislice imaging used for parenchymal imaging.

A practical application of the importance of this balance of TE, motion-compensation gradients, and hardware limitations can be found when smaller fields of view (FOVs) are used for intracranial MRA. Depending on the system hardware, reducing the FOV for intracranial MRA from 20 cm to 14 cm to improve resolution (while keeping the velocity compensation) may place such demands on the gradients that the TE must be increased. A typical TE for a 20-cm FOV might be 6.5 msec, but this may increase to 8 msec when the smaller 14-cm FOV is used. Again, the gradient “gas” is limited by the system hardware, and this gas can go toward a smaller FOV or a very short TE but not both. Even this seemingly small change of 1.5 msec can